

Effectively Rearranging Heterogeneous Objects on Cluttered Tabletops

Kai Gao Justin Yu Tanay Sandeep Punjabi Jingjin Yu

Abstract—Effectively rearranging heterogeneous objects constitutes a high-utility skill that an intelligent robot should master. Whereas significant work has been devoted to the grasp synthesis of heterogeneous objects, little attention has been given to the planning for sequentially manipulating such objects. In this work, we examine the long-horizon sequential rearrangement of heterogeneous objects in a tabletop setting, addressing not just generating feasible plans but near-optimal ones. Toward that end, and building on previous methods, including combinatorial algorithms and Monte Carlo tree search-based solutions, we develop state-of-the-art solvers for optimizing two practical objective functions considering key object properties such as size and weight. Thorough simulation studies show that our methods provide significant advantages in handling challenging heterogeneous object rearrangement problems, especially in cluttered settings. Real robot experiments further demonstrate and confirm these advantages.

Source code and evaluation data associated with this research will be available at <https://github.com/arc-1/TRLB> upon the publication of this manuscript.

I. INTRODUCTION

In pick-n-place-based multi-object rearrangement problems, a robot is tasked to move objects, generally one at a time, from a start arrangement to a desired goal arrangement. Multi-object rearrangement is a fundamental robotic task in commercial, domestic, and many other settings. In supermarkets, a robot can assist in maintaining organized shelves. At home, a robot can be utilized for tasks such as cleaning up kids’ rooms or reorganizing a messy desk.

Among rearrangement problems, Tabletop Object Rearrangement with Overhand grasps (TORO) has been extensively studied due to its many applications to real-world scenarios. The apparently simple setup is in fact NP-hard to optimally solve [1]. The difficulty is due to the overlaps between the start and goal arrangements, which makes it impossible to directly move some objects to the goal poses before some other objects are first moved away. For example, in Fig. 1[Right], the white bag cannot move to the goal pose before the black mug moves away from the current pose. When many such dependencies exist, they entangle and give rise to a combinatorial challenge. Deciding the best sequence to untangle the dependencies and minimize the total number of temporarily displaced objects makes the problem NP-hard.

In addition to the combinatorial challenge of minimizing the total number of displaced objects, another potentially more thorny issue in solving TORO is finding ideal locations

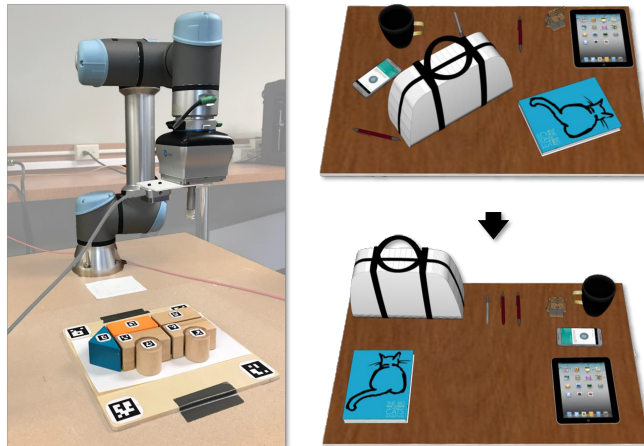


Fig. 1. [Left] Our hardware setup for evaluating tabletop rearrangement of multiple heterogeneous objects. One of the test cases is also shown. [Right] The illustration of an example instance where many objects of drastically different sizes and weights are to be rearrangements.

(i.e., *buffers*) for temporarily placing objects that cannot be directly moved to their goals. This issue appears when the workspace is cluttered with limited free space. In the example from Fig. 1[Right], the book and the phone cannot move to the goal pose before the other object is moved away, so at least one of these two objects needs to be moved to a *buffer* to break the mutual dependency. Suppose we are limited to using the tabletop as the workspace, it is not immediately clear which object should be moved away and where within the tabletop the moved object should be temporarily displaced. We denote this subclass of TORO as TORI (a TORO in which temporarily displaced objects must remain *internal* to the tabletop workspace) [2].

Until now, algorithmic research on TORI is limited to solving instances with mostly homogeneous objects [1]–[4]. The assumption of homogeneous objects leads to a relatively simple model where each object manipulation action has the same or very similar cost, which in turn limits the applicability of the resulting methods. In many real-world tabletop rearrangement problems, objects are often heterogeneous. For example, in Fig. 1, some objects are small and thin, e.g., pens, while others can be bulky, e.g., the white bag. Intuitively, objects’ sizes and shapes impact the rearrangement planning process - it is more difficult to relocate larger objects temporarily. Furthermore, other properties, such as weight, affect the effort needed to move them around. This further complicates the computation of optimal rearrangement plans. We thus ask a natural question here: Can we leverage objects’ properties to guide multi-object rearrangement planning?

All authors are with the Department of Computer Science, Rutgers, the State University of New Jersey, Piscataway, NJ, USA.

This work is partly supported by NSF awards IIS-1845888 and IIS-2132972, and an Amazon Research Award.

With the question in mind, we investigate heterogeneous TORI (HeTORI), in which the characteristics of workspace objects, such as size, shape, weight, and other properties, can vary significantly. Taking object characteristics into consideration immediately leads to a much more general problem model, allowing each manipulation operation to have a cost that is affected by the properties of the objects. For example, manipulating an object that is large, heavy, and/or fragile is naturally more challenging. As a result, such an operation could take more time to complete. Therefore, a higher cost may be given for such operations than manipulating an object that is small, light, and/or tough. This work focuses on developing methods taking into account such differences. More specifically, we develop methods for addressing two problem variants. In one of the variants, object shape and size are considered in generating the manipulation plan. Object characteristics are directly reflected in the optimization objective in the other variant.

In studying HeTORI, we deliver the following results and contributions:

- The formulation and investigation of the HeTORI problem, to our knowledge, is a first in introducing significant object heterogeneity in long-horizon manipulation task planning, adding not only generality but also additional computational complexity. In contrast, previous object rearrangement research generally assumes uniform objects and/or uniform manipulation costs.
- We examine *optimally* solving HeTORI over two practical objectives, with one assuming uniform manipulation costs but taking into account object heterogeneity and the other directly associating manipulation costs with object heterogeneity, i.e., larger objects take longer to move around. For both objectives, we develop SOTA methods based on deterministic and Monte Carlo tree search that greatly enhance computational efficiency and solution optimality, particularly for cluttered settings.
- Thorough simulation studies show that considering object heterogeneity translates into better plans for solving HeTORI, compared with approaches ignoring individual objects' differences. Real robot experiments further confirm these findings.

Paper Organization The rest of the paper is organized as follows. We first provide an overview of previous works in related fields in Sec. II. In Sec. III, we formally present the studied problem HeTORI. Then, in Sec. IV, we describe algorithmic approaches used to solve HeTORI. In Sec. V, we evaluate the performance of our proposed methods. Finally, we present our conclusion in Sec. VI.

II. RELATED WORK

Robotic manipulation [5] can be categorized into prehensile (e.g., [6], [7]) or non-prehensile (e.g., [8]–[11]) methods. Non-prehensile manipulations, e.g., pushes or pokes, are simple to execute but less predictable. Prehensile manipulations, on the other hand, result in more precise movements that facilitate long-horizon planning. Object rearrangement

is widely applicable to diverse scenarios. The most typical ones are tabletop [4], [7], [12] and shelf setups [6], [13], [14] with fixed robot arms. Larger environments with mobile robots [15]–[17] have also been examined. Typical rearrangement problems seek plans to move objects to desired goal positions, some variations, e.g., NAMO (Navigation Among Movable Obstacles) [18] or object retrieval problems [19]–[22], clear out a path to relocate a target object or the robot among movable obstacles.

In TORO, object collisions due to overlaps between the start and goal arrangements can be encoded into a dependency graph, which connects the rearrangement problem to established graph problems [1], [23], [24]. With the dependency graph, efficient algorithms and structural properties have been obtained for TORO. Specifically, assuming external space for temporary placements, the challenge of TORO embeds NP-hard Feedback Vertex Set (FVS) problem and Traveling Salesperson Problem (TSP) [1].

Our previous work [23] studies another natural objective for TORO, minimizing the number of *running buffers*, which is the number of currently displaced objects (in some space external to the workspace). It turns out that the running buffer objective can effectively help free space management in cluttered workspaces, leading to a speedy and high-quality method, TRLB (Tabletop Rearrangement with Lazy Buffers), for solving TORO problems [2], [24]. Besides dependency graph-based methods, there are some recent works on TORO utilizing reinforcement learning models [25]–[28] and Monte Carlo Tree Search (MCTS) [3]. In examining TORO with heterogeneous objects, this work boosts the performance of the dependency graph-based method TRLB and the MCTS-based method with the aid of object characteristics.

The study of manipulating heterogeneous objects is generally limited to the grasp synthesis of single objects [29]–[31]. With the aid of powerful simulators, recent works synthesize grasps by ranking sampled candidate grasps [32] or using data-driven methods [33], [34]. In addition to the challenge of searching for reachable grasps, for unknown objects, grasp poses are sampled based on local or global shape features identified from the sensing data [35], [36]. To our knowledge, sequential manipulation planning of heterogeneous objects has received little attention. In this research, we investigate effective ways to leverage object properties to guide the rearrangement planning of heterogeneous objects.

III. PRELIMINARIES

In this section, we formally define HeTORI. We then explain the dependency graph structure and Tabletop Rearrangement with Lazy Buffers (TRLB), a method for TORI. An alternative method [3] based on Monte Carlo Tree Search [37] is also briefly explained.

A. Heterogeneous TORI (HeTORI)

Consider a bounded rectangular tabletop workspace $\mathcal{W} \subset \mathbb{R}^2$ in front of a robot arm. The robot arm can reach every point on \mathcal{W} . There is a set of n objects $\mathcal{O} = \{o_1, o_2, \dots, o_n\}$

in \mathcal{W} . Each object o_i , $1 \leq i \leq n$, is an upright generalized cylinder. The generalized cylinder assumption, together with the overhand grasp/release, implies that the effective object pose space is $SE(2)$. A pose $p_i = (x, y, \theta) \in SE(2)$ for object o_i is *valid* if o_i at p_i is inside \mathcal{W} and does not collide with other objects at their current poses. Otherwise, we say pose p_i is *in collision* (with some pose p_j for some object o_j). An object arrangement $\mathcal{A} = \{p_1, p_2, \dots, p_n\}$ is *feasible* if all the poses in \mathcal{A} are valid poses. We consider overhand pick-n-places for object manipulation. Each pick-n-place a can be represented as (o_i, p_i) , where the robot arm R grasps o_i at the current pose from above, lifts it up, moves it horizontally over a valid pose p_i , and finally places it down. The task is to compute a *rearrangement plan*, which is a sequence of pick-n-places $\Pi = \{a_1, a_2, \dots, a_{|\Pi|}\}$ moving objects one at a time from a feasible start arrangement \mathcal{A}_s to a feasible goal arrangement \mathcal{A}_g .

HeTORI assumes full knowledge of object characteristics $\mathcal{I} = \{I_1, I_2, \dots, I_n\}$. \mathcal{I} may include properties of objects, including geometry, mass, material properties, and so on. In practice, \mathcal{I} can be estimated based on sensing data.

On a tabletop, a pick-n-place action consists of object grasp/release and end-effector travel. In the vanilla version of TORO, it is typically assumed that the time required for the end-effector to move is negligible compared to the time needed for grasping and releasing objects. Therefore, the quality of rearrangement plans can be evaluated based on the total number of grasps (and an equal number of releases) in solving a task. For HeTORI, if the robot is sufficiently powerful, it may still be the case that grasping/releasing objects takes the same amount of time for each object, regardless of their sizes and mass (with some range); but it could also be that different objects requires different (time) cost to grasp/release. Based on the observation, for HeTORI, two cost objectives are examined in this study, which are:

- 1) **(PP)** Total number of relocations, i.e., $J(\Pi) = |\Pi|$.
- 2) **(TI)** Total task *impedance*, i.e.,

$$J(\Pi) = \sum_{(o_i, p_i^1, p_i^2) \in \Pi} f(I_i). \quad (1)$$

Specifically, the PP objective is the number of grasps or places a robot needs to execute in a rearrangement plan. The TI objective enables the prioritization of manipulation actions based on objects' intrinsic properties, where $f(I_i)$ represents the actual cost of manipulating object o_i , as determined by the robot and I_i . Compared to PP, the TI objective represents the manipulation cost with higher levels of fidelity. For example, if a robot is tasked to rearrange gold and iron bars of the same size and shape, it is certainly better to move iron bars more due to iron's significantly lower density.

Based on the descriptions so far, HeTORI can be formally summarized as follows:

Problem 1 (HeTORI). *Given two feasible arrangements \mathcal{A}_s and \mathcal{A}_g of objects \mathcal{O} , compute a rearrangement plan Π moving \mathcal{O} from \mathcal{A}_s to \mathcal{A}_g with the minimum cost $J(\Pi)$.*

B. Dependency Graph

In TORO, due to pose collisions between the start and goal arrangements, some objects cannot be moved to goal poses before others are moved away. This leads to *dependencies* among objects. Specifically, we say an object o_i *depends on* another object o_j if the goal pose of o_i intersects (collides with) the start pose of o_j . Based on object dependencies, we construct a *dependency graph* \mathcal{G} to guide the task planning process for in TORO. In \mathcal{G} , each vertex v_i represents an object o_i , and there is an arc from v_i to v_j if o_i depends on o_j . \mathcal{G} encodes pose collisions between the start and goal arrangements. Fig. 2 shows the corresponding dependency graph of the TORO instance in Fig. 1.

When a dependency graph is acyclic, objects can be moved directly to the goal poses following the topological order. When the dependency graph contains cycles, some objects must be relocated to “break the cycles” before other objects in the cycles and themselves can be moved to the goal poses. The benefits of using the dependency graph \mathcal{G} are threefold: First, \mathcal{G} contains the information for computing the least number of object relocations to complete the rearrangement. For example, in Fig. 2, removing the book vertex from \mathcal{G} breaks all three cycles in \mathcal{G} , which suggests temporarily displacing the book to a collision-free buffer pose. Second, the strongly connected components in \mathcal{G} help decouple the rearrangement problem. In Fig. 2, there is one 5-vertex component and four single-vertex components. We can solve the subproblem induced by each component individually, which helps reduce the problem scale when dealing with many objects. Third, \mathcal{G} pre-computes collisions between start and goal arrangements. In general rearrangement problems, at each timestep, most of the objects are either at start poses or goal poses. Therefore, referring to \mathcal{G} saves much time on collision detection efforts.

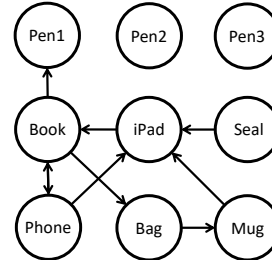


Fig. 2. The corresponding dependency graph of for the TORO (and also a HeTORI) instance from Fig. 1.

C. Tabletop Rearrangement with Lazy Buffers (TRLB)

The dependency graph \mathcal{G} suggests a decoupling of the rearrangement problem and a set of objects moved to buffers but it cannot suggest collision-free buffer poses for these objects inside the workspace. To solve TORI, TRLB (Tabletop Rearrangement with Lazy Buffers) [2] uses \mathcal{G} to guide the rearrangement planning process. TRLB computes a rearrangement plan in two steps. First, it computes a sequence of primitive actions, each of which indicates an object to move to either a buffer pose or the corresponding goal pose. In the example of Fig. 1, a primitive action can be a command like

“move the book to a buffer” or “move Pen3 to the goal”. After that, in the second step, for objects that need buffers, TRLB searches for buffer poses not colliding with other objects or blocking later primitive actions. When the two-step strategy fails, TRLB records a partial rearrangement plan and conducts a bi-directional search to concatenate partial plans into a complete plan. TRLB efficiently computes high-quality plans and is shown to be effective in solving dense instances when objects are homogeneous.

For primitive plan computation, TRLB provides two options: TBM (total buffer minimization) and RBM (running buffer minimization). TRLB with TBM computes primitive plans minimizing the total number of primitive actions moving objects to the buffers. TBM is equivalent to computing the minimum feedback vertex set of the dependency graph \mathcal{G} , a set of vertices in \mathcal{G} whose removal makes \mathcal{G} acyclic. The optimal solution of TBM can be obtained via dynamic programming or integer programming [1], [23]. This option seeks the shortest primitive plan but is not scalable to the number of objects and workspace density levels (how cluttered the workspace is) due to the computational complexity and the neglect of the difficulty of buffer allocation. TRLB with RBM computes primitive plans minimizing the maximum number of objects concurrently staying at buffer poses. RBM can be computed by DFDP (depth-first dynamic programming), a method of performing exhaustive state space search in a depth-first manner. It is a more efficient alternative to TBM but may return slightly longer primitive plans.

D. MCTS for Solving TORI

Labbe et. al. [3] propose a Monte Carlo Tree Search (MCTS) based method for TORI. Each state in MCTS represents an arrangement of objects. At each state, an action a_i either moves object o_i to the goal pose or relocates an object blocking o_i 's goal pose to a collision-free pose. The reward is the number of objects at goals. MCTS selects actions based on the upper confidence bound (UCB):

$$\operatorname{argmax}_a \left(\frac{\omega(f(s, a))}{n(f(s, a))} \right) + C \sqrt{\frac{2 \log(n(s))}{n(f(s, a))}}, \quad (2)$$

where $f(s, a)$ is the resulting state from state s after an action a , $n(s)$ and $\omega(s)$ represent the number of times that state is visited and the total rewards after the visits of s . In Eq.2, the first term is an exploration term, representing the expected rewards after action a , and the second term is the exploitation term, prioritizing the actions with fewer visits.

IV. METHODOLOGY

Our algorithmic design methodology is general: different (weighting) heuristics can be employed by different search strategies (e.g., TRLB and MCTS) for solving HeTORI. Here, we first describe our carefully constructed heuristics that are applicable to both PP and TI objectives. Then, for TRLB, we construct a weighted dependency graph with the heuristics and formulate the corresponding feedback vertex

set problem and running buffer minimization problem. For MCTS, we use the heuristics with additional improvements.

A. Weighting Heuristics

1) *Collision Probability (HeCP) for PP*: In a cluttered workspace, it is difficult to allocate collision-free poses for use as buffers. Even when a pose is collision-free in the current arrangement, it may overlap/collide with some goal poses, blocking the movements of other objects. It is generally more challenging to allocate high-quality buffers for objects with large sizes or aspect ratios (e.g., stick-like objects). A natural question would be: How much do the object's size and shape impact its collision probability with other objects? We compute an estimated collision probability for each object to answer the question. Based on the collision probability, we propose a heuristic HeCP (Heterogeneous object Collision Probability) to address the buffer allocation challenge in HeTORI and guide the rearrangement search.

Given two objects A and B with fixed orientations, positions of B colliding with A can be represented by the *Minkowski difference* of the two objects. That is,

$$A \ominus B(0, 0) := \{a - b | a \in P_A, b \in P_B(0, 0)\},$$

where P_A is the point set of A at the current pose and P_B is the point set of B at position $(0, 0)$ with the current orientation. Note that when B is rotational symmetric, the Minkowski difference is the same as the Minkowski sum, which replaces the minus with a plus in the formula above.

Specifically, for a convex polygon P and a disc D , the area of $P \ominus D(0, 0)$ can be simply represented as $S_N = S_P + S_D + r_D C_P$, where S and C are the area and circumference of corresponding objects, r_D is the radius of D .

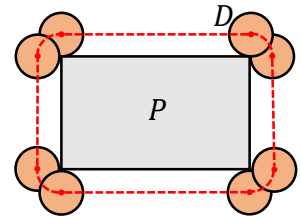


Fig. 3. An illustration of the Minkowski difference $P \ominus D(0, 0)$ (red dashed region) of a rectangle P and a disc D .

In the example of Fig. 3, S_P comes from the polygon P in the center of N , S_D comes from the four rounded corners, and $r_D C_P$ comes from the area along the edges. Since one of the objects is a disc, the formula is rotation invariant. Furthermore, if P is at least $2r_D$ away from the boundary of \mathcal{W} , the probability of D colliding with P is

$$\Pr = \frac{S_N}{(H - 2r_D)(W - 2r_D)} = \frac{S_P + S_D + r_D C_P}{(H - 2r_D)(W - 2r_D)} \quad (3)$$

Assuming both P and D are small compared to \mathcal{W} , \Pr is a fairly tight upper bound of the collision probability of P and D in the workspace.

Based on Eq. 3, the HeCP heuristics can be computed as in Algo. 1. The algorithm consumes the object characteristics \mathcal{I} . We first compute the area and circumference of each object based on \mathcal{I} (Lines 1-4). In Lines 5-6, we create a disc whose size is the average size of workspace objects. The area and radius of the average-sized disc are denoted as \bar{s} and \bar{r} , respectively. The weight of each object is then computed as the estimated collision probability between the

object and the average-sized disc (Lines 7-9).

In general, HeCP measures the difficulty of allocating a collision-free pose for an object and the probability of the sampled pose blocking other objects’ movements.

Algorithm 1: HeCP

Input : \mathcal{L} : object characteristics.

Output: HeCP: weights on \mathcal{O}

```

1 for  $o_i \in \mathcal{O}$  do
2    $s_i \leftarrow \text{getSize}(I_i)$ 
3    $c_i \leftarrow \text{getCircumference}(I_i)$ 
4 end
5  $\bar{s} = (\sum_{1 \leq i \leq n} s_i) / n$ 
6  $\bar{r} = \sqrt{\bar{s} / \pi}$ 
7 for  $o_i \in \mathcal{O}$  do
8    $w_i \leftarrow \frac{s_i + \bar{s} + \bar{r}c_i}{(H - 2\bar{r})(W - 2\bar{r})}$ 
9 end
10 return  $\{w_1, w_2, \dots, w_n\}$ 

```

2) *Task Impedance (HeTI) for TI:* When task impedance is evaluated, directly applying the existing methods, which seek rearrangement plans with the minimum number of actions, may lead to undesirable sub-optimality. For the TI objective, the weighting heuristic is denoted as HeTI. HeTI gives each object o_i a weight $f(I_i)$ as defined in Eq. (1).

B. Extended TRLB (ETRLB) for HeTORI

Recall that TRLB first computes a primitive plan and then allocates buffers to check plan feasibility. For HeTORI, we leverage weighting heuristics to guide the primitive plan computation in TRLB, which yields to *Extended TRLB* (ETRLB). To do so, we first construct a weighted dependency graph \mathcal{G}_w , where each vertex v_i has a weight w_i . Correspondingly, in the primitive plan computation process, we solve weighted TBM and weighted RBM of \mathcal{G}_w . For convenience, we use the notations ETBM and ERBM to represent ETRLB with weighted TBM and RBM, respectively. ETBM computes a primitive plan minimizing the total weights of objects moving to buffers. We transform the problem into computing the feedback vertex set of \mathcal{G}_w with the minimum sum of weights, which can be solved by dynamic programming or integer programming similar to TBM in TRLB. The same as the TRLB with RBM, ERBM computes the minimum running buffer size for the rearrangement problem but it assumes each object o_i to take w_i amount of space in buffers.

In the original RBM computation, TRLB fixes the running buffer size and checks whether there is a feasible rearrangement plan given the running buffer size in order to make use of the efficiency of depth-first search. If not, the algorithm increases the running buffer size by one and checks the feasibility again. This process continues until it finds the lowest running buffer size with a feasible primitive plan. Since this framework needs an integer running buffer size,

ERBM rounds the weights to the nearest integers so that the sum of weights is still an integer.

For HeTORI with the PP objective, applying HeCP in primitive plan computation discourages relocation of objects for which the allocation of high-quality buffers is difficult, which reduces the challenge in the buffer allocation process. When weighting heuristic HeCP is used, ETBM and ERBM seek primitive plans minimizing the total amount of “difficulty on buffer allocation” and the maximum “concurrent difficulty on buffer allocation”. For the TI objective, we apply HeTI to primitive plan computation instead.

C. Extended MCTS (EMCTS) for HeTORI

We also propose Extended Monte Carlo Tree Search (EMCTS) for heterogeneous instances. Specifically, for HeTORI with the PP objective, EMCTS applies HeCP to the exploration term in the UCB function, replacing constant C with

$$C(1 + \frac{w_i}{\sum_{i=1}^n w_i}).$$

EMCTS prioritizes actions making progress in sending high-weight objects to the goals (moving them to goals or clearing out their goal poses). We do this for two reasons. First, as mentioned in Sec. IV-A, it is difficult to move objects with high HeCP weights to buffers. And their allocated buffers are more likely to block other objects’ goal poses. Second, these high-weighted objects at goal poses are guaranteed to be collision-free from other goal poses. For HeTORI with the TI objective, the reward in EMCTS is the total HeTI weights of objects in the goal poses.

Besides the application of weighting heuristics, to tackle the challenge in HeTORI, we introduce two additional improvements to both MCTS and EMCTS.

1) *Reducing action space:* For each state, we only consider actions a_i whose corresponding object o_i are away from goal poses. This modification significantly reduces the action space when the state is close to the goal state and will not lead to optimality loss since the neglected actions will not make any difference to the workspace.

2) *Efficient collision checker for HeTORI:* In TORI, MCTS spends most of the computation time on collision checks for buffer allocation and goal pose feasibility checks. The original paper [3] uses the bounding discs for collision checks. For HeTORI, our collision checker has two steps: in the broad phase, we check collisions between bounding discs of object poses, which aims at pruning out most objects in the workspace that are far from the target object. In the narrow phase, for objects whose bounding discs overlap with that of the target object, we check the collision of their polygonal approximations. We also tried other broad-phase collision checkers, such as quadtrees and uniform space partitions. While these methods have good performance in large-scale collision checking, we observe limited speed-up but a large amount of overhead in maintaining the structures in HeTORI instance. That is because few robotic manipulation instances need to deal with more than 100 objects simultaneously.

V. EVALUATION

The proposed algorithms’ performance is evaluated using simulation and real robot experiments. All methods are implemented in Python, and the experiments are executed on an Intel® Xeon® CPU at 3.00GHz. Each data point is the average of 50 cases except for unfinished trials, given a time limit of 600 seconds per case.

A. Numerical Results in Simulation

Simulation experiments are conducted in two scenarios:

- 1) (RAND) In the RAND (random) scenario, for each object, the base shape is randomly chosen between an ellipse and a rectangle. The aspect ratios and the areas are uniformly random values in $[1.0, 3.0]$ and $[0.05, 1]$, respectively. The areas of the objects are then normalized to a certain sum S , whose value depends on specific problem setups. Examples of the RAND scenario are shown in the first row of Fig. 4. This setup is used to examine algorithm performance in general HeTORI instances.
- 2) (SQ) In the SQ (squares) scenario, there are 2 large squares and $|\mathcal{O}| - 2$ small squares. The area ratio between the large and small squares is 9 : 1. This setup simulates the rearrangement scenario where object size varies significantly. Examples of arrangements in the SQ scenario are shown in the second row of Fig. 4.

For each test case, object start and goal poses are uniformly sampled in the workspace for both scenarios. The sampling process for a single test case is repeated in the event of pose collision until a valid configuration is obtained. We use the *density level* ρ to measure how cluttered a workspace is. It is defined as $(\sum_{o_i \in \mathcal{O}} S_i) / S_W$, where S_i and S_W represents the size of o_i and the workspace respectively. In other words, ρ represents the proportion of the workspace occupied by objects. Fig. 4 shows examples of RAND and SQ scenarios for $\rho = 0.2-0.4$, where $\rho = 0.4$ is already fairly dense (e.g., 3rd column Fig. 4). We limit the maximum number of objects in a test case to 40 as typical HeTORI cases are unlikely to have more objects.

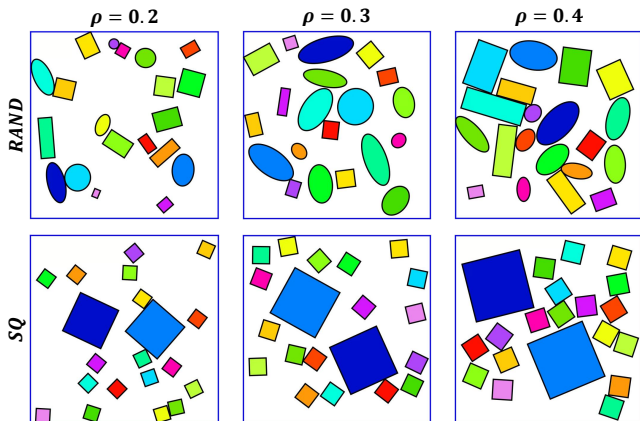


Fig. 4. Illustrations of some simulation test cases at different densities. [top] RAND instances under different density levels. [bottom] SQ instances under different density levels.

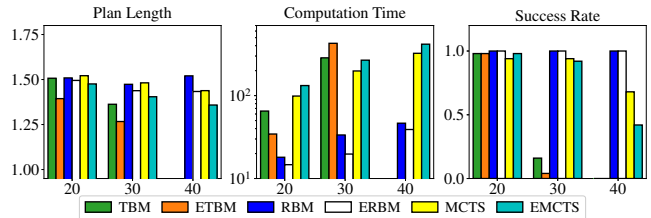


Fig. 5. Algorithm performance in RAND instances with $\rho = 0.4$ and 20-40 objects. [Left] Plan length as multiples of $|\mathcal{O}|$. [Middle] Computation time (secs). [Right] Success rate.

In Fig. 5, we first evaluate algorithm performance in dense RAND instances ($\rho = 0.4$) under the PP objective. Compared with the original TBM, ETBM shows a 7.8% improvement in solution quality with only 52% computation time, when both TBM and ETBM have 98% success rates in 20-object instances. Suffering from the expansion of solution space, neither TBM or ETBM is scalable as the number of objects increases. With HeCP, both ERBM and EMCTS show clear advantages compared to the original methods (RBM and MCTS) in solution quality as the number of objects increases. In 40-object instances, plans computed by ERBM and EMCTS save 3.6 and 3.2 actions over those by RBM and MCTS, respectively. While ERBM spends less time than RBM to solve RAND instances, EMCTS spends slightly more time on computation since the weights are added to the exploration term. In general, ETBM computes solutions with the best quality in small-scale instances, ERBM is most scalable as $|\mathcal{O}|$ increases, and EMCTS balances between optimality and scalability, computing high-quality solutions in 30-object instances with a high success rate.

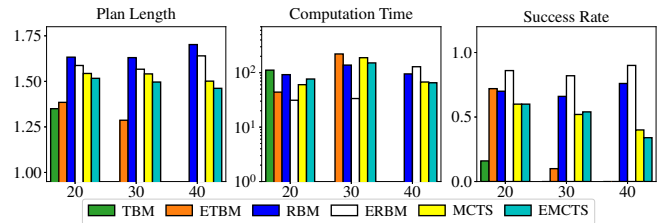


Fig. 6. Algorithm performance in SQ instances with $\rho = 0.4$ and 20-40 objects. [Left] Plan length as multiples of $|\mathcal{O}|$. [Middle] Computation time (secs). [Right] Success rate.

In SQ instances, it is difficult to displace the large squares in the cluttered workspace. Fig. 6 shows the algorithm performance in SQ instances with $\rho = 0.4$ under the PP objective. The results suggest that ETBM with HeCP effectively increases the success rate from 16% to 72% when $|\mathcal{O}| = 20$. Similarly, the success rate of ERBM is around 15% higher than RBM when $|\mathcal{O}| = 20, 30$, and 40. While ERBM solves more test cases, the computed solutions are even 5% – 7% shorter than RBM. As for MCTS methods, EMCTS computes 3% – 5% shorter paths than MCTS with a similar success rate and computation time.

Besides dense instances, we also evaluate the efficiency gain of HeCP at different density levels when $|\mathcal{O}| = 20$. The results of RAND and SQ scenarios are shown in Fig. 7 and Fig. 8 respectively. In sparse RAND instances ($\rho = 0.2$ or 0.3), ETBM and ERBM return plans with similar optimality

without additional computational overheads. When $\rho = 0.3$, EMCTS spends additional 5 seconds for exploration and receives around 3% improvements on path length.

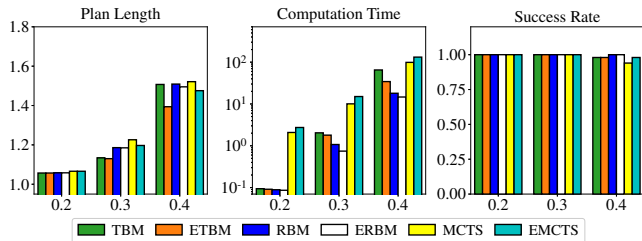


Fig. 7. Algorithm performance in RAND instances under different density levels and $|\mathcal{O}| = 20$. [Left] Plan length as multiples of $|\mathcal{O}|$. [Middle] Computation time (secs). [Right] Success rate.

In sparse SQ instances, HeCP helps improve computation time, which contributes to an increase in success rate. Compared with TBM, ETBM saves 70% computation time when $\rho = 0.2$ and 0.3 and increases the success rate from 82% to 98% when $\rho = 0.2$. Similarly, compared with RBM, ERBM saves 56% and 82% computation time when $\rho = 0.2$ and 0.3. In ETBM and ERBM, HeCP speeds up computation without reducing solution quality. Compared with MCTS, EMCTS computes 5% shorter plans, saves 33% computation time, and increases the success rate by 16% when $\rho = 0.3$.

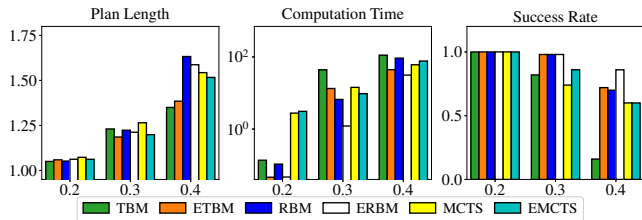


Fig. 8. Algorithm performance in SQ instances under different density levels and $|\mathcal{O}| = 20$. [Left] Plan length as multiples of $|\mathcal{O}|$. [Middle] Computation time (secs). [Right] Success rate.

In Fig. 9 and Fig. 10, we show the algorithm performance of HeTORI with TI objective in RAND and SQ instances respectively. $\rho = 0.3$ in the test cases. In RAND instances, where only around 10% objects need buffer locations, the total task impedance of computed plans is similar. Compared with original methods (TBM, RBM, and MCTS), ETBM, ERBM, and EMCTS reduce task impedance by 1% – 7%. In SQ instances, object impedance varies greatly. In this case, methods with HeTI compute much better solutions. Compared with TBM, ETBM reduce task impedance by over 30%. Similarly, ERBM reduces task impedance by around 27%. Compared with MCTS, EMCTS reduces task impedance by 6% – 15% but with additional overhead.

B. Demonstrations in Simulation and Real-World

In the accompanied video, we further demonstrate that our algorithms can be applied to practical instances with general-shaped objects in both simulation and the real world. For simulation instances, the rearrangement plans are executed in Pybullet. For real-world instances, the objects are detected with an Intel RealSense D405 RGB-D camera and manipulated with an OnRobot VGC 10 vacuum gripper on a

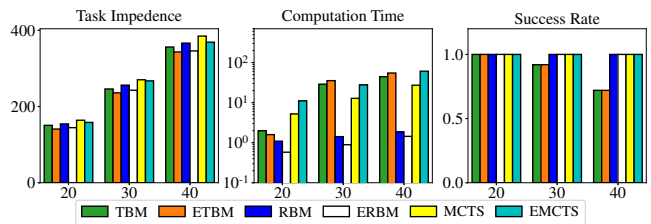


Fig. 9. Algorithm performance in RAND instances with TI objective. $\rho = 0.3$, $20 \leq |\mathcal{O}| \leq 40$. [Left] Total task impedance. [Middle] Computation time (secs). [Right] Success rate.

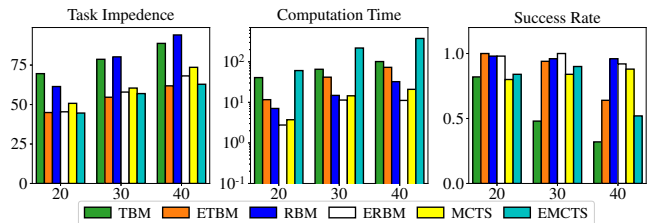


Fig. 10. Algorithm performance in SQ instances with TI objective. $\rho = 0.3$, $20 \leq |\mathcal{O}| \leq 40$. [Left] Total task impedance. [Middle] Computation time (secs). [Right] Success rate.

UR-5e robot arm. Since object recognition and localization are not the focus of this study, we use fiducial markers for realizing these. The workspaces for rearrangement are rather confined (in Fig. 11, the white areas for the first two and the wooden board for the third), translating to very high object densities, between 35–37%. In the SQ instance with 10 wooden planks, our proposed methods ETBM and ERBM offer advantages over TBM and RBM in both solution quality and computation time, saving 1 and 4 actions, respectively. Furthermore, EMCTS is able to find a 15-action plan in just 13.70 secs while MCTS fails to find a solution even after 2 minutes of computation.

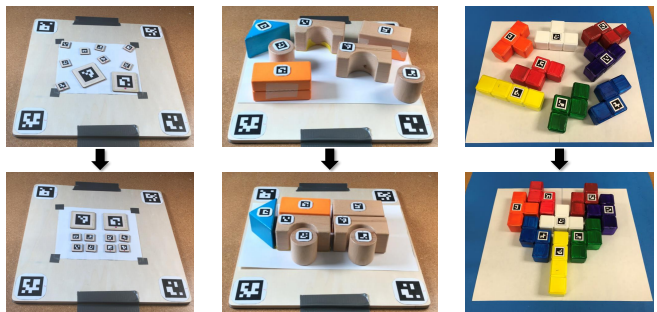


Fig. 11. Physical experiment/demo setups. [left] Dense SQ instance with 10 square wooden planks. [middle] Rearranging densely-packed thick wooden blocks of different shapes and sizes. [right] Rearranging 3d-printed Tetris pieces into a heart shape.

VI. CONCLUSIONS

In this work, we examine rearranging heterogeneous objects on a tabletop (HeTORI) using two different objectives: PP and TI. The PP objective assumes each object requires an equal amount of manipulation cost for a pick-n-place, while utilizing the object’s shape and size can enhance rearrangement efficiency. On the other hand, the TI objective evaluates the total task impedance, where the manipulation

cost of each object varies based on its specific characteristics, such as size or weight. To optimize these objectives, we propose weighting heuristics and build SOTA algorithms with them. Extensive simulation experiments confirm the efficiency of our proposed methods. Moreover, we demonstrate the effectiveness of our methods in challenging real-world HeTORI instances through multiple demonstrations on a physical robot platform.

REFERENCES

- [1] S. D. Han, N. M. Stiffler, A. Krontiris, K. E. Bekris, and J. Yu, "Complexity results and fast methods for optimal tabletop rearrangement with overhand grasps," *The International Journal of Robotics Research*, vol. 37, no. 13-14, pp. 1775–1795, 2018.
- [2] K. Gao, D. Lau, B. Huang, K. E. Bekris, and J. Yu, "Fast high-quality tabletop rearrangement in bounded workspace," in *2022 International Conference on Robotics and Automation (ICRA)*. IEEE, 2022, pp. 1961–1967.
- [3] Y. Labbé, S. Zagoruyko, I. Kalevtykh, I. Laptev, J. Carpentier, M. Aubry, and J. Sivic, "Monte-carlo tree search for efficient visually guided rearrangement planning," *IEEE Robotics and Automation Letters*, vol. 5, no. 2, pp. 3715–3722, 2020.
- [4] R. Shome, K. Solovey, J. Yu, K. Bekris, and D. Halperin, "Fast, high-quality dual-arm rearrangement in synchronous, monotone tabletop setups," in *Algorithmic Foundations of Robotics XIII: Proceedings of the 13th Workshop on the Algorithmic Foundations of Robotics*. Springer, 2020, pp. 778–795.
- [5] Z. Pan, A. Zeng, Y. Li, J. Yu, and K. Hauser, "Algorithms and systems for manipulating multiple objects," *IEEE Transactions on Robotics*, vol. 39, no. 1, pp. 2–20, 2023.
- [6] R. Wang, Y. Miao, and K. E. Bekris, "Efficient and high-quality prehensile rearrangement in cluttered and confined spaces," in *2022 International Conference on Robotics and Automation (ICRA)*. IEEE, 2022, pp. 1968–1975.
- [7] K. Gao and J. Yu, "Toward efficient task planning for dual-arm tabletop object rearrangement," in *2022 IEEE/RSJ International Conference on Intelligent Robots and Systems (IROS)*. IEEE, 2022, pp. 10425–10431.
- [8] E. Huang, Z. Jia, and M. T. Mason, "Large-scale multi-object rearrangement," in *2019 International Conference on Robotics and Automation (ICRA)*. IEEE, 2019, pp. 211–218.
- [9] S. D. Han, B. Huang, S. Ding, C. Song, S. W. Feng, M. Xu, H. Lin, Q. Zou, A. Boularias, and J. Yu, "Toward fully automated metal recycling using computer vision and non-prehensile manipulation," in *2021 IEEE 17th International Conference on Automation Science and Engineering (CASE)*. IEEE, 2021, pp. 891–898.
- [10] H. Song, J. A. Haustein, W. Yuan, K. Hang, M. Y. Wang, D. Kragic, and J. A. Stork, "Multi-object rearrangement with monte carlo tree search: A case study on planar nonprehensile sorting," in *2020 IEEE/RSJ International Conference on Intelligent Robots and Systems (IROS)*. IEEE, 2020, pp. 9433–9440.
- [11] B. Huang, S. D. Han, A. Boularias, and J. Yu, "Dipn: Deep interaction prediction network with application to clutter removal," in *2021 IEEE International Conference on Robotics and Automation (ICRA)*. IEEE, 2021, pp. 4694–4701.
- [12] M. Danielczuk, A. Mousavian, C. Eppner, and D. Fox, "Object rearrangement using learned implicit collision functions," in *2021 IEEE International Conference on Robotics and Automation (ICRA)*. IEEE, 2021, pp. 6010–6017.
- [13] R. Wang, K. Gao, J. Yu, and K. Bekris, "Lazy rearrangement planning in confined spaces," in *Proceedings of the International Conference on Automated Planning and Scheduling*, vol. 32, 2022, pp. 385–393.
- [14] K. Wada, S. James, and A. J. Davison, "Reorientbot: Learning object reorientation for specific-posed placement," in *2022 International Conference on Robotics and Automation (ICRA)*. IEEE, 2022, pp. 8252–8258.
- [15] J. Gu, D. S. Chaplot, H. Su, and J. Malik, "Multi-skill mobile manipulation for object rearrangement," in *Deep Reinforcement Learning Workshop NeurIPS 2022*.
- [16] C. Gan, S. Zhou, J. Schwartz, S. Alter, A. Bhandwadar, D. Gutfreund, D. L. Yamins, J. J. DiCarlo, J. McDermott, A. Torralba, *et al.*, "The threedworld transport challenge: A visually guided task-and-motion planning benchmark towards physically realistic embodied ai," in *2022 International Conference on Robotics and Automation (ICRA)*. IEEE, 2022, pp. 8847–8854.
- [17] A. Szot, A. Clegg, E. Undersander, E. Wijnmans, Y. Zhao, J. Turner, N. Maestre, M. Mukadam, D. S. Chaplot, O. Maksymets, *et al.*, "Habitat 2.0: Training home assistants to rearrange their habitat," *Advances in Neural Information Processing Systems*, vol. 34, pp. 251–266, 2021.
- [18] M. Stilman and J. J. Kuffner, "Navigation among movable obstacles: Real-time reasoning in complex environments," *International Journal of Humanoid Robotics*, vol. 2, no. 04, pp. 479–503, 2005.
- [19] B. Huang, S. D. Han, J. Yu, and A. Boularias, "Visual foresight trees for object retrieval from clutter with nonprehensile rearrangement," *IEEE Robotics and Automation Letters*, vol. 7, no. 1, pp. 231–238, 2021.
- [20] J. Ahn, C. Kim, and C. Nam, "Coordination of two robotic manipulators for object retrieval in clutter," in *2022 International Conference on Robotics and Automation (ICRA)*. IEEE, 2022, pp. 1039–1045.
- [21] E. R. Vieira, D. Nakhimovich, K. Gao, R. Wang, J. Yu, and K. E. Bekris, "Persistent homology for effective non-prehensile manipulation," in *2022 International Conference on Robotics and Automation (ICRA)*. IEEE, 2022, pp. 1918–1924.
- [22] E. R. Vieira, K. Gao, D. Nakhimovich, K. E. Bekris, and J. Yu, "Persistent homology guided monte-carlo tree search for effective non-prehensile manipulation," *arXiv preprint arXiv:2210.01283*, 2022.
- [23] K. Gao, S. W. Feng, and J. Yu, "On running buffer minimization for tabletop rearrangement," in *17th Robotics: Science and Systems, RSS 2021*. MIT Press Journals, 2021.
- [24] K. Gao, S. W. Feng, B. Huang, and J. Yu, "Minimizing running buffers for tabletop object rearrangement: Complexity, fast algorithms, and applications," *The International Journal of Robotics Research*, p. 02783649231178565, 2023.
- [25] W. Yuan, J. A. Stork, D. Kragic, M. Y. Wang, and K. Hang, "Rearrangement with nonprehensile manipulation using deep reinforcement learning," in *2018 IEEE International Conference on Robotics and Automation (ICRA)*. IEEE, 2018, pp. 270–277.
- [26] W. Yuan, K. Hang, D. Kragic, M. Y. Wang, and J. A. Stork, "End-to-end nonprehensile rearrangement with deep reinforcement learning and simulation-to-reality transfer," *Robotics and Autonomous Systems*, vol. 119, pp. 119–134, 2019.
- [27] F. Bai, F. Meng, J. Liu, J. Wang, and M. Q.-H. Meng, "Hierarchical policy for non-prehensile multi-object rearrangement with deep reinforcement learning and monte carlo tree search," *arXiv preprint arXiv:2109.08973*, 2021.
- [28] K. N. Kumar, I. Essa, and S. Ha, "Graph-based cluttered scene generation and interactive exploration using deep reinforcement learning," in *2022 International Conference on Robotics and Automation (ICRA)*. IEEE, 2022, pp. 7521–7527.
- [29] A. Bicchi and V. Kumar, "Robotic grasping and contact: A review," in *Proceedings 2000 ICRA. Millennium conference. IEEE international conference on robotics and automation. Symposia proceedings (Cat. No. 00CH37065)*, vol. 1. IEEE, 2000, pp. 348–353.
- [30] J. Bohg, A. Morales, T. Asfour, and D. Kragic, "Data-driven grasp synthesis—a survey," *IEEE Transactions on robotics*, vol. 30, no. 2, pp. 289–309, 2013.
- [31] A. Sahbani, S. El-Khoury, and P. Bidaud, "An overview of 3d object grasp synthesis algorithms," *Robotics and Autonomous Systems*, vol. 60, no. 3, pp. 326–336, 2012.
- [32] M. Przybylski, T. Asfour, and R. Dillmann, "Planning grasps for robotic hands using a novel object representation based on the medial axis transform," in *2011 IEEE/RSJ International Conference on Intelligent Robots and Systems*. IEEE, 2011, pp. 1781–1788.
- [33] R. Newbury, M. Gu, L. Chumbley, A. Mousavian, C. Eppner, J. Leitner, J. Bohg, A. Morales, T. Asfour, D. Kragic, *et al.*, "Deep learning approaches to grasp synthesis: A review," *arXiv preprint arXiv:2207.02556*, 2022.
- [34] D. Morrison, P. Corke, and J. Leitner, "Closing the loop for robotic grasping: A real-time, generative grasp synthesis approach," *arXiv preprint arXiv:1804.05172*, 2018.
- [35] C. Wang, X. Zhang, X. Zang, Y. Liu, G. Ding, W. Yin, and J. Zhao, "Feature sensing and robotic grasping of objects with uncertain information: A review," *Sensors*, vol. 20, no. 13, p. 3707, 2020.
- [36] D. Fischinger, M. Vincze, and Y. Jiang, "Learning grasps for unknown objects in cluttered scenes," in *2013 IEEE international conference on robotics and automation*. IEEE, 2013, pp. 609–616.

- [37] L. Kocsis and C. Szepesvári, “Bandit based monte-carlo planning,” in *Machine Learning: ECML 2006: 17th European Conference on Machine Learning Berlin, Germany, September 18-22, 2006 Proceedings 17*. Springer, 2006, pp. 282–293.